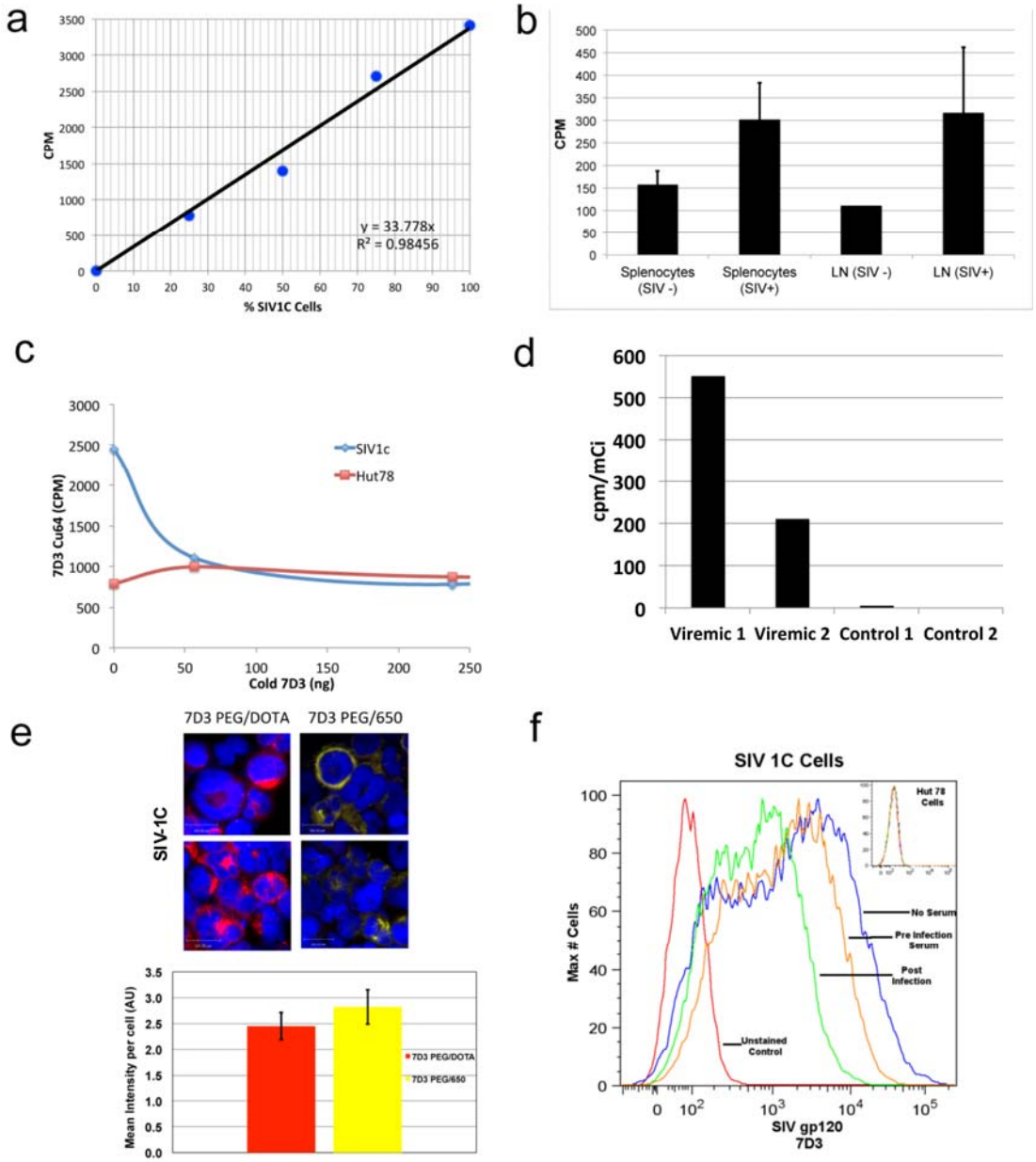

Supplementary Figure 1

In vitro binding of modified mAb clone 7D3 to SIV gp120, interrogated by scintillation counter, fluorescence microscopy and flow cytometry.

a. Counts per minute from 7D3-PEG-^{64}Cu-DOTA labeled SIV-1C serially diluted with Hut78 (non-infected) cells, demonstrating a linear response in samples with equal cell numbers. **b**. Counts per minute from cryopreserved and thawed splenocytes and lymph node cells, originating from uninfected and SIV infected animals collected at necropsy. The data demonstrates that even after a freeze-thaw cycle the 7D3-PEG- ^{64}Cu-DOTA probe binds specifically to infected cells. Shown are means and standard deviations from lymph node and spleen cells from 2 and 1 uninfected controls and 3 and 5 infected monkeys, respectively. **c**. Competition assay where unlabeled “cold”-7D3 was used to compete 200 ng bound “hot” 7D3-PEG-^{64}Cu-DOTA from SIV-1C and Hut78 cells, demonstrating epitope-specific binding of the probe. **d**. Probe bound virus pelleted from infected (Viremic 1 and Viremic 2) versus non-infected (Control 1 and Control 2) animal plasmas, 24 hrs post contrast agent injection, measured in counts per minute normalized to the dose given to each

animal. This demonstrates that at 24 hrs post injection, the probe is still stable, and can bind to its target specifically. **e**. Representative images of 7D3-PEG-DOTA (modified 7D3) and 7D3-PEG-Dylight 650 binding to SIV-1C cells, demonstrating specific binding. No statistical difference was found between the two probes. No signal was detected for either probe in Hut78 control cells (data not shown). This experiment demonstrates that the 650 labeled fluorescent probe binds with the same efficacy than the 7D3-PEG-DOTA (cold) probe. **f**. Flow cytometry profiles of 7D3-PEG-Dylight 650 binding to control cells, SIV-1C cells, and SIV-1C cells in the presence of pre-infection and post-infection serum. While both pre and post infection serum appear to compete with 7D3 binding to the infected cells, specific signal is still clearly seen relative to binding to uninfected cells.

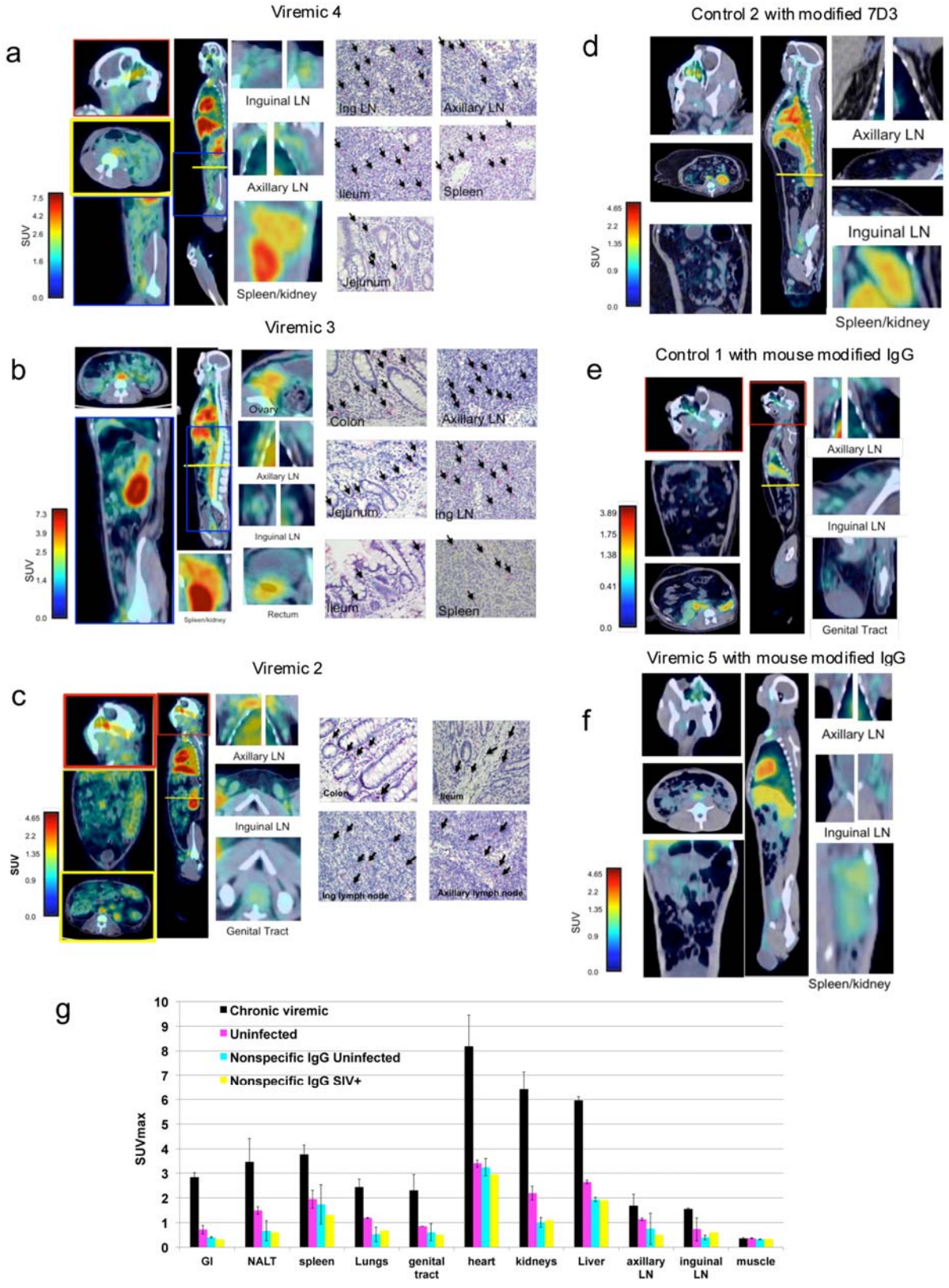
a
Viremic 4
Inguinal LN
Ing LN
Axillary LN
Axillary LN
Ileum
Spleen
Jejunum
Spleen/kidney
SUV
7.5
4.2
2.6
1.6
0.0
b
Viremic 3
Ovary
Colon
Axillary LN
Axillary LN
Jejunum
Ing LN
Inguinal LN
Rectum
Ileum
Spleen
Spleen/kidney
SUV
7.3
3.9
2.5
1.4
0.0
c
Viremic 2
Axillary LN
Colon
Ileum
Inguinal LN
Ing lymph node
Axillary lymph node
Genital Tract
SUV
4.65
2.2
1.35
0.9
0.0
d
Control 2 with modified 7D3
Axillary LN
Inguinal LN
Spleen/kidney
SUV
4.65
2.2
1.35
0.9
0.0
e
Control 1 with mouse modified IgG
Axillary LN
Inguinal LN
Genital Tract
SUV
3.89
1.75
1.38
0.41
0.0
f
Viremic 5 with mouse modified IgG
Axillary LN
Inguinal LN
Spleen/kidney
SUV
4.65
2.2
1.35
0.9
0.0
g
Chronic viremic
Uninfected
Nonspecific IgG Uninfected
Nonspecific IgG SIV+
SUVmax
10
9
8
7
6
5
4
3
2
1
0
GI
NALT
spleen
Lungs
genital tract
heart
kidneys
Liver
axillary LN
inguinal LN
muscle

Supplementary Figure 2

Additional PET and CT results from chronically SIV-infected viremic and control macaques.

a, b, c. Frontal, sagittal and axial views are presented, as well as magnified views (marked by a colored box and associated image denoted by the same color outline) of regions of the frontal and sagittal sections. The site corresponding to the axial section is identified within the sagittal view by a yellow line, while the sagittal view location, if not centerline, is denoted by a blue line in the frontal view. Single plane PET/CT cross-sections from macaques, Viremic 2-4, (for plasma viral loads see Supplementary Table 1) scanned at 24 hrs post injection of the contrast agent. Both animals demonstrated PET signals within the GI tract, including the ileum, jejunum, and colon, as well as within axillary and inguinal lymph nodes, and lungs. SIVgag p27 specific IHC for select organs of macaques Viremic 2-4, are also presented. Infected mononuclear cells (black arrows) were detected in the ileum, jejunum, and colon, as well as within lymph nodes and the spleen, verifying the PET results. **d**. Single plane images of modified 7D3 within non-infected macaque, Control 2. The sagittal image is taken from the centerline and the axial view is denoted by the yellow line within the sagittal view. The 7D3 probe did not yield significant uptake within the gut, axillary, mesenchymal, or inguinal lymph nodes. Background uptake was highest within the liver, heart, kidneys and spleen, as expected, though the signals measured in these organs were markedly lower than those quantified from the same organs in SIV infected monkeys, suggesting specific uptake above background in the infected animals. **e**. Control monkey number 1 given a modified isotype control IgG antibody; background signal detected was significantly lower than in the infected animals, even within the liver, heart, and kidneys, sites for which background was expected. **f**. Single plane images of modified mouse IgG within chronically-infected macaque, Viremic 5. Uptake was generally similar to the modified mouse IgG in the non-infected animals. **g**. SUVmax quantification for the chronically infected and non-infected animals, with the isotype control probe (modified mouse IgG) data in a chronically infected animal was added, demonstrating similar uptake to the non-infected animal.

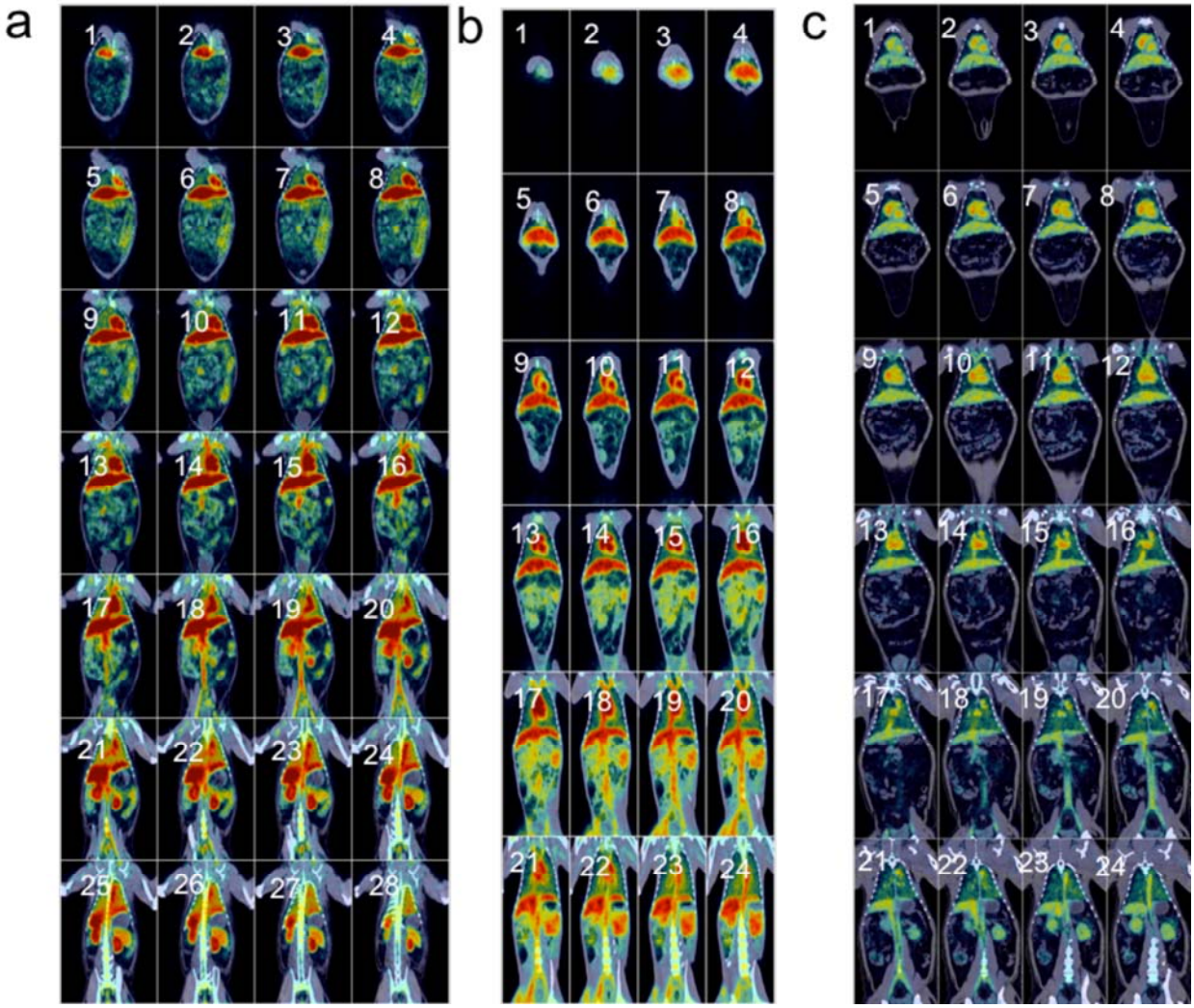

Supplementary Figure 3

Cross-sectional views of representative animals.

a. Cross-sections of the frontal torso and abdomen of SIV infected viremic monkey Viremic 2. Each slice is 1.37 mm thick; 28 slices are displayed, amounting to a frontal view every 2.74 mm. A SIV positive signal is apparent throughout the gastrointestinal tract, especially within the ileum, jejunum and colon, and within the lung. Background signal, as expected, was high within the liver, heart, and kidneys. **b**. Cross-sections of the frontal torso and abdomen of SIV infected viremic monkey Viremic 1. Each slice is 1.37 mm thick; 24 slices are displayed, amounting to a frontal view every 2.74 mm. A SIV positive signal is apparent throughout the GI tract and within the lung. Background signal, as expected, was high within the liver, heart, and kidneys. **c**. Cross-sections of the frontal torso and abdomen of uninfected monkey Control 1 given modified 7D3. In the frontal views, each slice is 0.98 mm thick, 24 slices are displayed, amounting to a frontal view every 1.96 mm. Very little signal above muscle background within the gastrointestinal tract, and lymph nodes. Background signal, as expected, was high within the liver, heart, and kidneys, and measurable within the lung.

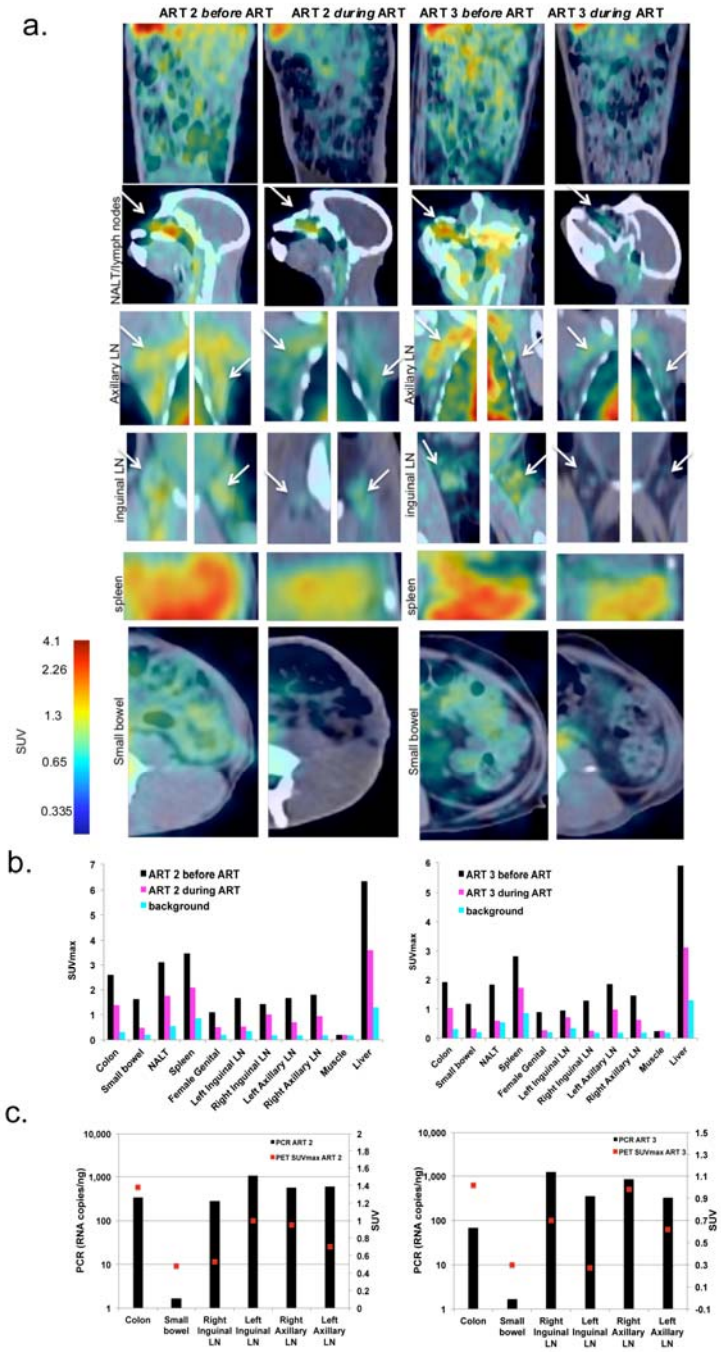

Supplementary Figure 4

PET-CT results from two additional chronically infected macaques, before and at 5 weeks of ART treatment.

PET/CT images of two SIV chronically infected macaques, ART 2 and 3, prior to and at 5 weeks of ART. **a**. Standard uptake value (SUV) maps of GI tract, lymph nodes, genital tract, spleen and small bowel, demonstrating decreased probe uptake after 5weeks of ART. **b**. SUVmax values before and after 5 weeks of ART, compared with background uptake in non-infected animals. **c**. qRT-PCR verification of residual virus compared with SUVmax PET data..

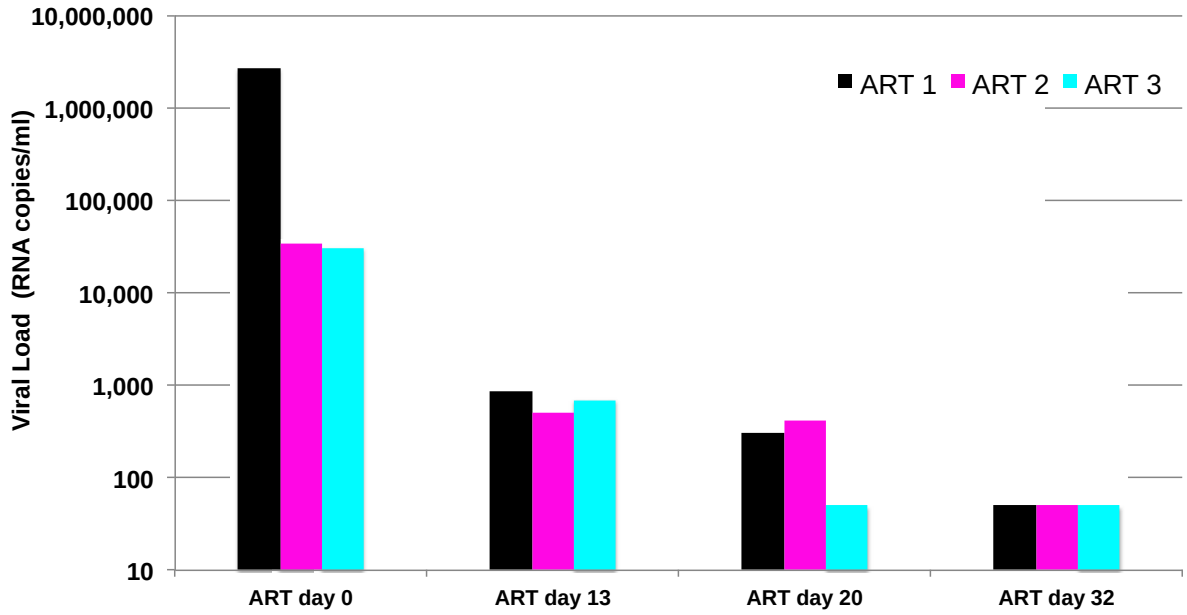

Supplementary Figure 5

Kinetics of plasma viral loads in the SIV-infected monkeys ART 1, 2 and 3, before and during ART.

All 3 monkeys were subjected to PET/CT analysis prior to ART initiation and again after 34 days on ART, before being euthanized on days 38/39 for tissue collections and analyses. By 3-4 weeks of ART, plasma viral loads were below the 60 copies/ml detection limit of the qRT-PCR assay.

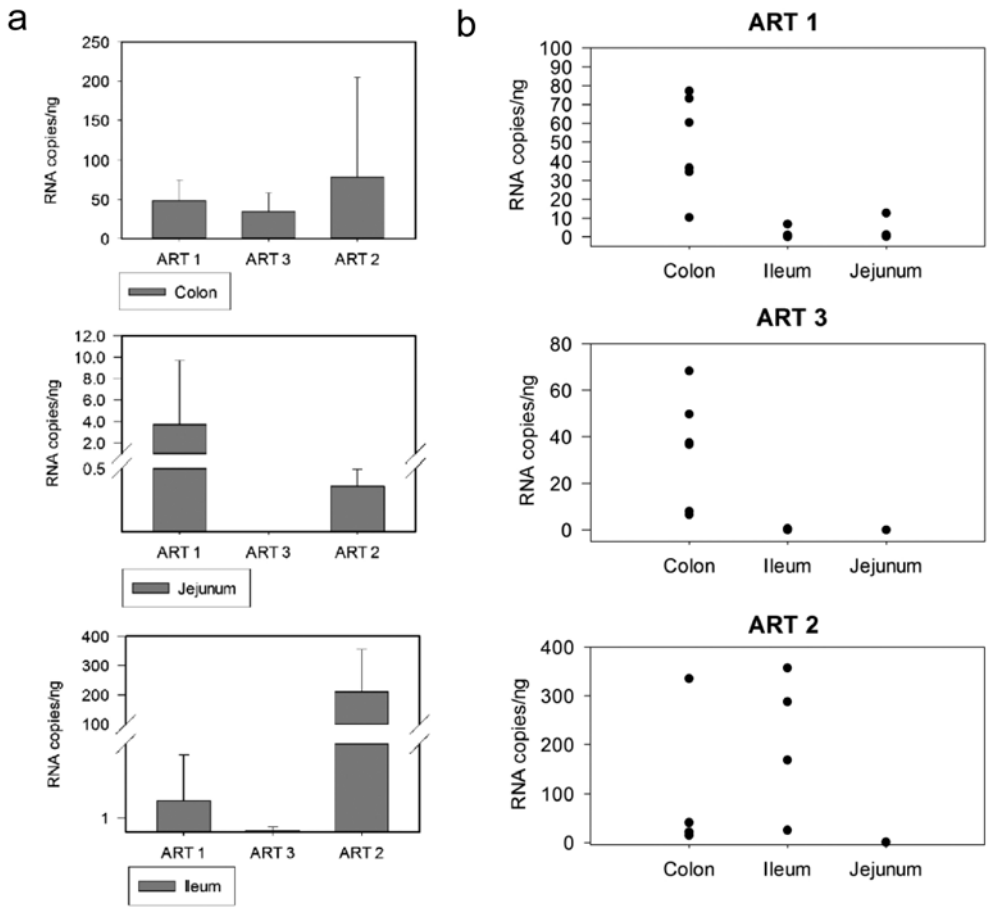

Supplementary Figure 6

Tissue viral loads in SIV-infected, ART-treated monkeys.

a. The average tissue viral loads (SIV vRNA copies/ng total RNA) were generated from 6 separate spatial samples for the colon, 4 for the jejunum and 4 for the ileum. The average viral loads were derived from the results of the 4-6 different sites collected and analyzed for each GI section. While average values for the colon were comparable for the 3 monkeys, there was far more variability (up to 2 orders of magnitude) in values obtained from the small bowel segments, suggesting potential differences in viral clearance during ART. In contrast, measuring gp120 via PET, an approximately 10-fold difference was observed between monkeys. **b**. These figures illustrate the differences in qRT-PCR signals obtained from various collection sites from the same GI segment of a given animal on ART. It is obvious from the data that the variation in viral RNA levels can range up to 2 orders of magnitude within the same tissue, especially for the colon. This clearly has implications for the interpretation of data obtained from biopsies relative to an entire organ. All qRT-PCR data is presented also in Supplementary Table 3.

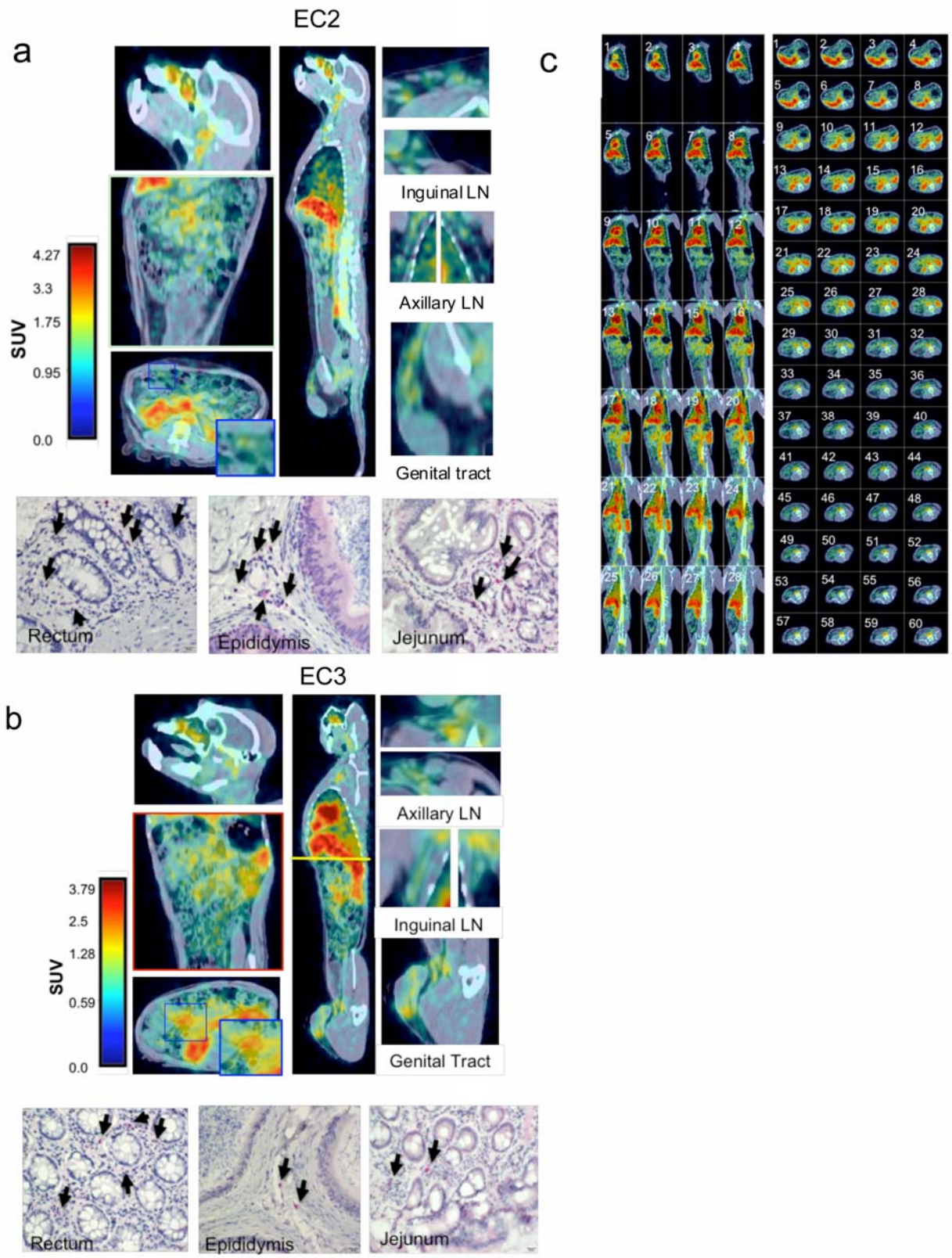

Supplementary Figure 7

Additional PET-CT results from an EC SIV-infected macaque.

a,b. Frontal, sagittal and axial views are presented, as well as magnified views (marked by a colored box and associated image denoted by the same color outline) of regions of the frontal and sagittal sections. Single plane PET/CT cross-sections from macaque EC 2 and 3, 36 hrs post injection of the contrast agent. EC 2 and 3 demonstrated PET signal foci in the GI tract, including the ileum, jejunum, and colon, as well as within axillary, mesenteric, and inguinal lymph nodes, and male genital tract. IHC for p27 Gag results from biopsy samples for each monkey are also presented. Infected mononuclear cells (black arrows) were detected in the rectum, epididymis and jejunum, verifying the PET results. **b**. Cross-sections of frontal and axial views of macaque EC 3, an elite controller. For the frontal views, each slice is 1.37 mm thick, 24 slices are displayed, amounting to a frontal view every 5.46 mm. The axial view thickness is 5 mm and images are displayed every 3 mm. SIV positive signal is apparent throughout the GI tract, and within the lung. Background signal, as expected, was high within the liver, heart, and kidneys.

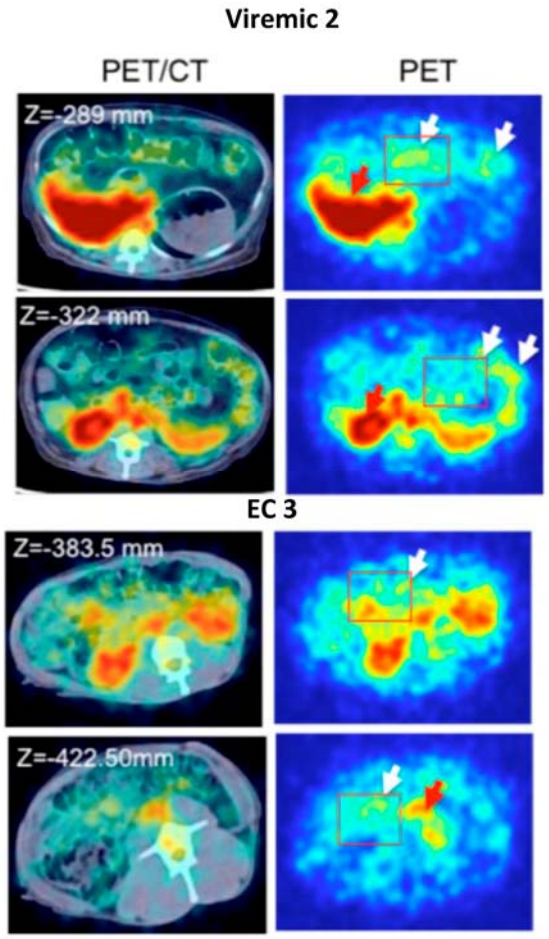

Supplementary Figure 8

Comparison of PET signal distribution in viremic and EC macaques.

Representative axial cross sections of chronically infected macaques (Viremic 2) and controller macaques (EC3). The uptake in the chronically viremic infected animals (white arrows) tend to follow the length of the GI organs, while in the controllers (white arrows), the signal localizes to specific foci, some of which are mesenteric lymph nodes (from CT), while in other cases they correspond to specific regions of the small intestines or colon. The red arrows indicate uptake within the liver.

Additional supplementary information

Monkeys	Yerkes designation	sex	age years	Body Weight kg	Dose mCi	Time pi Weeks	Mamu alleles A*001/B*008/B*017	SIV plasma VL mRNA/ml	Clinical status
Viremic 1	RFR-11	M	5	6.9	1.2	69	- / - / -	1.65E+05	viremic
Viremic 2	RID-9	F	9	9.12	3.7	71	- / - / -	6.85E+05	viremic
Viremic 3	RLC-8	F	10	8.8	2.1	66	- / - / -	2.89E+05	viremic
Viremic 4	RCN-10	F	7	6	1	66	- / - / -	1.64E+06	viremic
Viremic 5	RYY13	M	4	7.46	3	34	+ / - / -	7.53E+04	viremic
EC 1	RUN-10	M	8	9.86	3	>6y	+ / - / -	< 60	EC
EC 2	RMP-10	M	8	14.48	1.8	>6y	- / - / -	< 60	EC
EC 3	RBQ-10	M	8	10.06	1.6	>6y	- / - / -	< 60	EC
EC 4	RQZ-8	F	10	7.75	1.3	112	+ / - / -	< 60	EC
ART 1	RUT-13	M	4	5.84	1	13	+ / - / -	2.64E+06	viremic *
ART 2	RHY-12	F	6	5.94	1	38	- / - / -	3.39E+04	viremic *
ART 3	RQM-11	F	8	8.48	1	37	- / - / -	3.06E+04	viremic *
ART 1	RUT-13	M	4	6.1	1	41	- / - / -	< 60	ART
ART 2	RHY-12	F	6	6	1	42	- / - / -	< 60	ART
ART 3	RQM-11	F	8	8.5	1	41	- / - / -	< 60	ART
Control 1	RHG-7	M	11	12.6	1.2	0	- / - / -	< 60	uninfected
Control 2	RVE-7	M	11	15.75	1.5	0	- / - / -	< 60	uninfected

viremic * = pre-ART

Supplementary Table 1. Macaques used in this study, including gender, weights, probe specific activity, time post-infection with SIV and viral load at the time of imaging.

Experiment 1: Chronic viremic vs Uninfected control vs Isotype control (24hrs)

	Organ	Kruskal-Wallis (SUVmax)
1	GI	0.0073
4	NALT	0.0073
5	spleen	0.0231
6	Lungs	0.0073
7	genital tract	0.0145
8	heart	0.0183
9	kidneys	0.0073
10	Liver	0.0073
11	axillary LN	0.0183
12	inguinal LN	0.0125
14	muscle	0.06

Experiment 2: EC vs Chronic viremic (36 hrs)

Organ		ANOVA (SUVmax)	Kruskal-Wallis (SUVmax)
1	GI	0.0089	0.0621
4	NALT	0.0173	0.0665
5	spleen	0.0004	0.0665
7	genital tract	0.0479	0.0509
8	heart	0.0006	0.0665
9	kidneys	0.0001	0.0273
10	Liver	0.0018	0.0509
11	axillary LN	0.0008	0.0273
12	inguinal LN	0.0498	0.0509
13	facial/cranial LN	0.0008	0.0665
14	muscle	0.0783	0.0594

Supplementary Table 2. Kruskal-Wallis analysis of the statistical differences in SUVmax measurements in individual organ systems, comparing animal status (infected viremic vs uninfected, ECs vs infected viremic). The data analyzed here is depicted in Figure 1 and 3. From this data it is clear that for all organ systems (yellow), the differences in PET signals are statistically significant ($p<0.05$) except for the muscle. For ECs vs viremic monkey comparisons, only the kidneys and axillary lymph nodes (yellow) showed a statistical difference in the SUVmax. However, differences were detected when using the SUVmean ($p<0.05$) (Figure 4) by the same statistical test.

a

Percent reduction in SUVmax after 4 weeks of ART						
	Colon	*Small bowel*	*NALT*	*spleen*	*testes*	*genital tract*
ART 1	64.36%	51.07%	43.67%	27.61%	72.78%	37.33%
ART 2	46.81%	69.94%	43.68%	40.36%	NA	53.64%
ART 3	50.71%	73.86%	70.11%	43.81%	NA	71.10%
AVERAGE	53.96%	64.96%	52.49%	37.26%	72.78%	54.02%
STDEV	9.21%	12.19%	15.26%	8.53%		16.89%

	left inguinal LN	*right inguinal LN*	*left axillary LN*	*right axillary LN*	*liver*
ART 1	47.31%	NA	68.32%	68.37%	29.55%
ART 2	68.27%	29.40%	58.02%	47.56%	43.36%
ART 3	64.23%	81.12%	51.16%	60.70%	51.41%
AVERAGE	59.94%	55.26%	59.16%	58.88%	41.44%
STDEV	11.12%	36.57%	8.64%	10.52%	11.06%

b

	ART 1 (viral copies per ngRNA)	ART 3 (viral copies per ngRNA)	ART 2(viral copies per ngRNA)
Mesenteric LN	2448.86	179.67	526.48
Right Inguinal LN	4104.47	1253.08	278.44
Left Inguinal LN	4440.32	353.65	1065.40
Right Axil LN	973.14	839.49	561.09
Left Axil LN	3749.70	325.57	602.91
Colon 1	60.42	68.32	14.47
Colon 2	36.61	6.54	15.15
Colon 3	10.32	7.92	41.11
Colon 4	73.07	49.65	40.38
Colon 5	77.01	37.30	21.49
Colon 6	34.56	36.63	335.37
Jejunum 1	0.21	Undetected	0.46
Jejunum 2	0.64	Undetected	0.48
Jejunum 3	12.67	Undetected	0.19
Jejunum 4	1.22	Undetected	0.31
Cecum	4.83	1.66	7.73
Ileum 1	6.75	0.49	356.88
Ileum 2	0.91	Undetected	168.07
Ileum 3	undetected	Undetected	25.18
Ileum 4	0.96	Undetected	287.61
Spleen	1824.07	64.07	58.09
Kidney R	2.53	0.06	0.17
Kidney L	23.81	0.18	0.41
Urethra	3.64	No sample	No sample
Testis	0.25	No sample	No sample
Epididymis	0.36	No sample	No sample
Saminal Gland	2.62	No sample	No sample
Prostate	0.79	No sample	No samples
Vagina	No sample	0.92	Undetected
Ectocervix	No sample	0.18	0.76
Endocervix	No sample	1.26	2.07
Uterus	No sample	0.08	Undetected
Ovary	No sample	0.01	Undetected
Lung 1	9.89	4.28	10.40
Lung 2	5.53	3.60	Undetected
Tonsil lingual	77.01	Undetected	63.72
Tonsil pharyngeal	7.43	80.88	365.97
Nasal turbinate	1.36	4.70	8.85

Supplementary Table 3. **a.** Percent reduction in SUVmax after 5 weeks of ART treatment of chronically infected macaques. **b.** Tissue qRT-PCR results of 3 monkeys chronically infected with SIV and sacrificed after 5 weeks of ART. At the time of sacrifice, all three animals were aviremic, with less than 60 copies vRNA/ml plasma. The data also illustrate the variability in the various samples and sites collected from the colon, jejunum, cecum, ileum, and lung, illustrating the spatial heterogeneity of SIV within organs from an animal. A portion of this data is plotted in Supplementary Fig. 6.

Supplementary Note 1. SIV localization in infected aviremic elite controller macaques. Once the sensitivity and specificity of the immunoPET/CT method was demonstrated, highlighted by its ability to distinguish uninfected from SIV infected ART treated animals, the approach was used to image SIV infected elite controllers (EC). ECs are individuals that maintain SIV or HIV replication levels to undetectable levels in plasma for extended periods of time without ART[1-3]. The study of the pathogenesis, viral persistence, and interventions in these individuals is challenging due to the absence of detectable plasma viremia. We reasoned that EC monkeys would serve as additional important candidates for an imaging technique that can identify potential sites of residual virus replication. Therefore, four macaques identified as ECs were injected with the 7D3 probe and imaged. In Figure 3, fused frontal, sagittal, and axial, PET/CT images from 1 of the 4 LTNPs, EC 1, is displayed, focusing on the nasal associated tissue, GI tract, inguinal/axillary lymph nodes and the genital tract. This animal had been infected with SIV >6 years with viral loads of <60 copies of viral RNA per ml of plasma for the last >5 years. The images of the controllers (Fig. 3 and Supplementary Figure 7) show similarities with those of the viremic animals, but also marked differences. They exhibited detectable uptake within the GI tract, genital tract (epididymis), NALT, lungs, spleen and axillary lymph nodes, but the signal was markedly more restricted to small foci within the positive organs. In addition to the images displayed in Figure 3, images from EC 2 (Supplementary Fig. 7a) and individual frontal and axial image slices throughout the entirety of EC 3 were studied and are displayed (see Supplementary Fig. 7b) providing a more detailed view of the anatomical localization of signals. The signal quantified using the SUVmax integration surprisingly provided levels comparable to those seen in viremic animals (Figure 3b). However, further analysis using the hierarchical ANOVA clearly showed that viremic animals were statistically distinct from the ECs, with a p-value of 2.78e-5, and while each population was distinct, individuals within viremic monkeys or ECs appeared homogenous ($\beta_{j(i)}$=0; p-value=0.9804). Individual organ differences were assessed by both Kruskal-Wallis with statistical differences in the kidneys and axillary lymph nodes or by ANOVA (with Bonferoni) where additional differences were detected (Supplementary Table 2). The imaging results were verified via IHC (Figure 3c and Supplementary Fig. 7a,b) assays performed on biopsies of the rectum, jejunum, and the epididymis. SIVgag$^+$ cellular infiltrates (black arrows) were detected in each of these tissues with the highest prevalence within jejunum and rectum, corroborating the PET imaging results. These animals were not sacrificed because they are part of a number of ongoing studies aimed at unraveling mechanism(s) by which these SIV infected animals maintain their EC status.

To further clarify and quantify the differences between ECs and viremic animals, the SUVmean was measured specifically within the GI tract (Figure 4a). In addition, the voxel fractions (fraction of total volume of GI tract) that contained SUVs above 1 and less than 3.3 (excludes interfering signals) were compared (Fig. 4a). Using the mean signal as a yardstick, it was found that the GI tract from the chronic SIV$^+$ viremic macaques exhibited 2.1 times the signal obtained on the ECs. Moreover, when the volume of tissue with uptake between 1 and 3.3 was examined, the chronic SIV$^+$ macaques exhibited 6.38 times the signal of the ECs. These data clearly demonstrate that while the viremic SIV$^+$ macaques and the ECs both contain regions of high uptake

with similar maximal intensity, the signal distribution is markedly different. In order to more quantitatively compare the variation in the signal distribution within regions of the GI tract, two Haralick texture features[4], the angular second moment and contrast were calculated for the same size ROI (Fig. 4b,c,d) within both chronically infected and elite controller animals. The angular second moment is a measure of homogeneity, while the contrast metric represents the local variations within an image or ROI. These metrics are inversely proportional to each other, and therefore ideal to compare the distributions of signal within the GI tract of SIV infected viremic animals and ECs. In Figure 4b, both metrics were plotted; the angular second moment for the chronically infected animals was 4.6X higher than in the ECs, while the contrast in the ECs was 8.4X higher than in the chronically viremic animals. These objective metrics clearly demonstrate that the signal within the GI tract of the SIV infected viremic animals is more homogeneous than the signal within the GI tract of the ECs, reflecting the conclusion that in ECs, the signal is located within foci or small regions. (Figure 3 and 4c,d).

References

1. Saez-Cirion A, Bacchus C, Hocqueloux L, Avettand-Fenoel V, Girault I, Lecuroux C, et al. Post-treatment HIV-1 controllers with a long-term virological remission after the interruption of early initiated antiretroviral therapy ANRS VISCONTI Study. PLoS Pathog. 2013; **9**(3): e1003211.
2. Grabar S, Selinger-Leneman H, Abgrall S, Pialoux G, Weiss L, Costagliola D. Prevalence and comparative characteristics of long-term nonprogressors and HIV controller patients in the French Hospital Database on HIV. AIDS. 2009; **23**(9): 1163-9.
3. Zaunders J, van Bockel D. Innate and Adaptive Immunity in Long-Term Non-Progression in HIV Disease. Front Immunol. 2013; **4**: 95.
4. Haralick RM, Shanmugam K, Dinstein I. Textural Features for Image Classification. IEEE Transactions on Systems, Man, and Cybernetics. 1973; **3**(6): 610-21.